Article

Quantitative and Comprehensive Decomposition of the Ion Atmosphere around Nucleic Acids

Yu Bai, Max Greenfeld, Kevin J. Travers, Vincent B. Chu, Jan Lipfert, Sebastian Doniach, and Daniel Herschlag

J. Am. Chem. Soc., **2007**, 129 (48), 14981-14988 • DOI: 10.1021/ja075020g

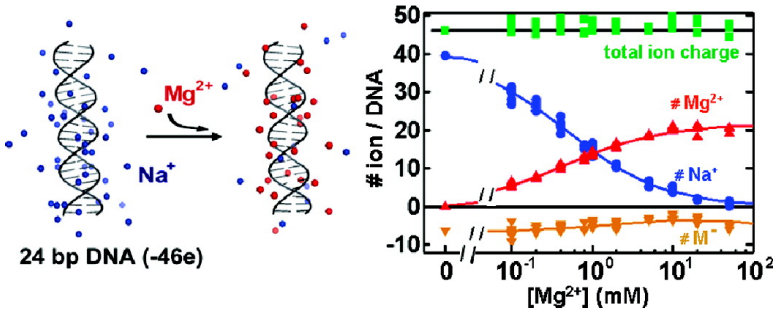

More About This Article

Additional resources and features associated with this article are available within the HTML version:

- Supporting Information
- Links to the 1 articles that cite this article, as of the time of this article download
- Access to high resolution figures
- Links to articles and content related to this article
- Copyright permission to reproduce figures and/or text from this article

View the Full Text HTML

J|A|C|S
ARTICLES
Published on Web 11/09/2007

Quantitative and Comprehensive Decomposition of the Ion Atmosphere around Nucleic Acids

Yu Bai,[†,‡] Max Greenfeld,[§,‡] Kevin J. Travers,[‡] Vincent B. Chu,[∥] Jan Lipfert,[⊥] Sebastian Doniach,[†,∥,⊥] and Daniel Herschlag*[,†,‡,§]

Contribution from the Biophysics Program and Departments of Biochemistry, Chemical Engineering, Applied Physics and Physics, Stanford University, Stanford, California 94305

Received July 6, 2007; E-mail: herschla@stanford.edu

Abstract: The ion atmosphere around nucleic acids critically affects biological and physical processes such as chromosome packing, RNA folding, and molecular recognition. However, the dynamic nature of the ion atmosphere renders it difficult to characterize. The basic thermodynamic description of this atmosphere, a full accounting of the type and number of associated ions, has remained elusive. Here we provide the first complete accounting of the ion atmosphere, using buffer equilibration and atomic emission spectroscopy (BE−AES) to accurately quantitate the cation association and anion depletion. We have examined the influence of ion size and charge on ion occupancy around simple, well-defined DNA molecules. The relative affinity of monovalent and divalent cations correlates inversely with their size. Divalent cations associate preferentially over monovalent cations; e.g., with Na^+ in 4-fold excess of Mg^{2+} (20 vs 5 mM), the ion atmosphere nevertheless has 3-fold more Mg^{2+} than Na^+. Further, the dicationic polyamine putrescine^{2+} does not compete effectively for association relative to divalent metal ions, presumably because of its lower charge density. These and other BE−AES results can be used to evaluate and guide the improvement of electrostatic treatments. As a first step, we compare the BE−AES results to predictions from the widely used nonlinear Poisson Boltzmann (NLPB) theory and assess the applicability and precision of this theory. In the future, BE−AES in conjunction with improved theoretical models, can be applied to complex binding and folding equilibria of nucleic acids and their complexes, to parse the electrostatic contribution from the overall thermodynamics of important biological processes.

1. Introduction

The polyelectrolyte nature of nucleic acids profoundly affects their behavior. Catalytic RNAs fold upon addition of cations, *in vitro* ribosome assembly is dictated by ionic conditions, and the association of proteins with DNA and RNA strongly depends on the ions present.[1−3] These strong dependencies arise because the negatively charged phosphoryl groups of a nucleic acid chain provide an enormous repulsion.[3−5] Indeed, the electrostatic repulsion experienced in folding a ∼400-nucleotide RNA or DNA molecule in the absence of counterions would be $\sim 10^3$ kcal/mol.[5] The specific association of cations with functional RNA molecules is important in folding and function and has received much attention.[6] However, the vast majority of cations that associate with a nucleic acid are part of a mobile sheath of ions surrounding the molecule, the "ion atmosphere" (Figure 1A).[3,7,8]

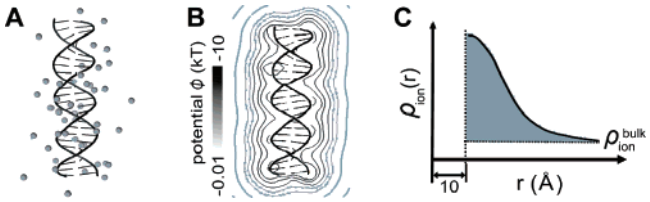

Figure 1. Ion atmosphere around nucleic acids. The formation of a condensed layer of counterions around the DNA (A) is driven by and in return modulates the negative electrostatic potential surrounding the DNA (Φ, B). In the PB model, the ion distribution, shown as a radial density function ($\rho_{ion}(r)$, (C)), is determined by the potential (Φ) at an indicated location via Boltzmann weighting.

The presence of the ion atmosphere is well-established, but the properties of and contributions from this environment have been difficult to decipher. In particular, the atmosphere has no discrete structure, rendering it impervious to structural techniques such as X-ray crystallography. Additionally, the atmosphere has complex thermodynamic behavior relative to simple site binding of a metal ion or other ligand. The properties that prevent its description in terms of simple binding isotherms have been clearly articulated by Misra and Draper.[9,10] Further, they

[†] Biophysics Program.
[‡] Department of Biochemistry.
[§] Department of Chemical Engineering.
[∥] Department of Applied Physics.
[⊥] Department of Physics.

(1) Woodson, S. A. *Curr. Opin. Chem. Biol.* **2005**, *9*, 104−109.
(2) Herrera, J. E.; Correia, J. J.; Jones, A. E.; Olson, M. O. *Biochemistry* **1996**, *35*, 2668−2673.
(3) Draper, D. E. *RNA* **2004**, *10*, 335−343.
(4) Jayaram, B.; Sharp, K. A.; Honig, B. *Biopolymers* **1989**, *28*, 975−993.
(5) Bai, Y.; Das, R.; Millett, I. S.; Herschlag, D.; Doniach, S. *Proc. Natl. Acad. Sci. U.S.A.* **2005**, *102*, 1035−1040.
(6) DeRose, V. J. *Curr. Opin. Struct. Biol.* **2003**, *13*, 317−324.
(7) Manning, G. S. *J. Chem. Phys.* **1969**, *51*, 924−933.
(8) Sharp, K. A.; Honig, B. *Curr. Opin. Struct. Biol.* **1995**, *5*, 323−328.
(9) Misra, V. K.; Draper, D. E. *J. Mol. Biol.* **1999**, *294*, 1135−1147.
(10) Misra, V. K.; Draper, D. E. *J. Mol. Biol.* **2000**, *299*, 813−825.

have demonstrated that RNA folding previously interpreted in terms of site binding of Mg^{2+} ions may instead be accounted for by occupancy of the ion atmosphere.[10]

The predominant description of the ion atmosphere arises from theory.[3,7,11,12] The early treatments such as counterion condensation theory by Manning articulated the critical concept of the ion atmosphere and provided an excellent first-order estimation of ion association.[7] Nevertheless, condensation theory employed simplifications and *ad hoc* assumptions in modeling the polyelectrolyte and its interactions with ions.[9] The currently widely used treatment is Poisson−Boltzmann (PB) theory that is developed from the fundamental electrostatic equations.[8,10,13] This theory describes the electrostatic potential surrounding a macromolecule and how that potential is modulated by the presence of different ion constituents and concentrations (Figure 1B).[8] Its mean-field approximation of the distribution of electrolytes and the continuum model for solvent render PB conceptually straightforward and computationally tractable. The availability of software routines to solve the nonlinear PB (NLPB) equation for complex biological systems has further led to the widespread application of PB.[10,13,14]

Nevertheless, there are limitations to NLPB theory. Ions are treated as point charges without discrete size. Thus, properties that arise because each ion excludes others from overlap in the same space are neglected.[15] Further, NLPB calculates a Boltzmann-weighted ion density at each position. This average ion density (Figure 1C) does not take into account correlations expected because the position of one ion influences the preferred position of other ions in the atmosphere.[16,17]

Although these limitations have been extensively discussed in theoretical treatments,[15−18] there has been no straightforward and rigorous experimental benchmark for comparison. Most fundamentally, comprehensive experimental data are lacking for a full thermodynamic description of the ion atmosphere, despite its clear importance in the structural behaviors and associations of nucleic acids. A large body of literature has determined the modulation of folding transitions and binding events of nucleic acids from changes in ion concentration (see refs 1 and 19 and the refs therein). However, the physical and electrostatic interactions between the macromolecule and ions are not directly addressed or distinguished in such experiments. Examining the equilibrium of a folding (or binding) process assays the difference in ion association with the folded and unfolded states; the absolute extent of the association with both states is not obtained. Moreover, the ion association in such folding and binding studies is often convoluted with conformational transitions, preventing straightforward analysis of effects from the ion atmosphere.[19] In addition, analyses to extract information from these experiments about the ion atmosphere have typically invoked simplifying assumptions that are valid only under limited conditions.[9,10,20,21] Thus, direct assessment of the ion atmosphere associated with molecules of a defined state is a critical early step in robustly determining the quantitative relationship between the ions and their energetic consequences.

There have been several experimental attempts to more directly assess the ion atmosphere by determining its content. While providing important information, each approach has significant limitations. $^{23}Na^+$ NMR line broadening arises from interactions of Na^+ ions with DNA,[22] but there is no strict relationship between this line broadening and the thermodynamic association of Na^+ ions in the ion atmosphere.[23] Dye-indicator methods can determine the amount of a target ion that is free in solution,[24−27] the decrease of free ions providing a strict thermodynamic measure of ions associated with DNA. However, dye association can be complex,[28] and only a subset of ions have appropriate indicator dyes. Gel electrophoresis measures the mobility of nucleic acids affected by the presence of ions and their distribution within the atmosphere, but such mobility data cannot be converted into a model-free description of the ion atmosphere.[29] Anomalous small-angle X-ray scattering (ASAXS)[30] provides incisive information about the ion distribution around a nucleic acid that is impervious to other techniques (including the technique developed herein). Nevertheless, it is not highly quantitative in terms of the number of ions bound and is limited in assay throughput and in the assayable ions. Mg^{2+} binding to tRNA has been accessed by equilibrating an ionic buffer with the tRNA-containing solution followed by atomic absorption spectroscopy to count the excess Mg^{2+} ions associated with the RNA.[31] This technique provides a true thermodynamic measure of ion binding. However, there is considerable experimental scatter in the atomic absorption data (see Results), and interpretation of these particular results is limited by the complexity of the tRNA structure with its conformational transitions and potential site binding of Mg^{2+} ions.

A better understanding of the ion atmosphere and its structural and energetic consequences requires an experimental approach that can directly and precisely measure the complete content of the ion atmosphere. High throughput data acquisition is also

(11) Pack, G. R.; Wong, L.; Lamm, G. *Biopolymers* **1999**, *49*, 575−590.
(12) Quesada-Perez, M.; Gonzalez-Tovar, E.; Martin-Molina, A.; Lozada-Cassou, M.; Hidalgo-Alvarez, R. *ChemPhysChem* **2003**, *4*, 234−248.
(13) Sharp, K. A.; Honig, B. *Annu. Rev. Biophys. Biophys. Chem*. **1990**, *19*, 301−332.
(14) Baker, N. A.; Sept, D.; Joseph, S.; Holst, M. J.; McCammon, J. A. *Proc. Natl. Acad. Sci. U.S.A.* **2001**, *98*, 10037−10041.
(15) Borukhov, I.; Andelman, D. *Phys. Rev. Lett.* **1997**, *79*, 435−438.
(16) Grosberg, A. Y.; Nguyen, T. T.; Shklovskii, B. I. *Rev. Mod. Phys.* **2002**, *74*, 329−345.
(17) Nishio, T.; Minakata, A. *J. Phys. Chem. B* **2003**, *107*, 8140−8145.
(18) Nishio, T.; Minakata, A. *J. Chem. Phys.* **2000**, *113*, 10784−10792.
(19) Misra, V. K.; Draper, D. E. *Biopolymers* **1998**, *48*, 113−135.
(20) Anderson, C. F.; Record, M. T. *Annu. Rev. Phys. Chem.* **1995**, *46*, 657−700.
(21) For salt-dependent folding or ligand-binding reactions, ion-binding isotherms have typically been fit to a polynomial binding model based on the simple mass action equilibrium. However, this equilibrium is not a physical description of the long-range electrostatic interactions governing the behavior of the ion atmosphere. Further, the exclusion of anions is typically neglected in these analyses, a condition that is only satisfied for very low salt concentration (0.01 M, refs 9, 20).
(22) Anderson, C. F.; Record, M. T. *Annu. Rev. Biophys. Biophys. Chem.* **1990**, *19*, 423−465.
(23) Some Na^+ ions in the atmosphere may be close enough to experience relaxation from the DNA but others may not be. Further, the ion distribution can change with ionic conditions. Quantitatively comparing results over a series of conditions is difficult.
(24) Grilley, D.; Soto, A. M.; Draper, D. E. *Proc. Natl. Acad. Sci. U.S.A.* **2006**, *103*, 14003−14008.
(25) Romer, R.; Hach, R. *Eur. J. Biochem.* **1975**, *55*, 271−284.
(26) Krakauer, H. *Biopolymers* **1971**, *10*, 2459−2490.
(27) Das, R.; Travers, K. J.; Bai, Y.; Herschlag, D. *J. Am. Chem. Soc.* **2005**, *127*, 8272−8273.
(28) Dye association has complex thermodynamics as neutral dye-indicators may bind to metal ions that are free or part of the ion atmosphere, although presumably there is partial or extensive exclusion of the dye-bound metal ion from the atmosphere because of the preference for smaller cations in the atmosphere.
(29) Li, A. Z.; Huang, H.; Re, X.; Qi, L. J.; Marx, K. A. *Biophys. J.* **1998**, *74*, 964−973.
(30) Das, R.; Mills, T. T.; Kwok, L. W.; Maskel, G. S.; Millett, I. S.; Doniach, S.; Finkelstein, K. D.; Herschlag, D.; Pollack, L. *Phys. Rev. Lett.* **2003**, *90*, 188103:1-4.
(31) Stein, A.; Crothers, D. M. *Biochemistry* **1976**, *15*, 157−160.

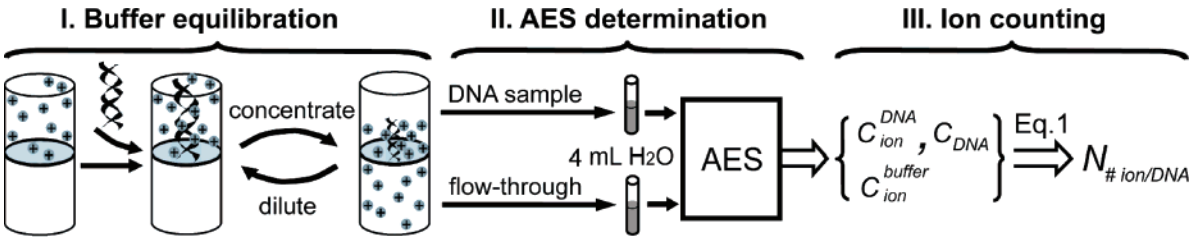

Figure 2. Scheme of the buffer equilibration−atomic emission spectroscopy (BE−AES) approach.

important as it allows comparisons of ion atmospheres for a variety of ions and molecules under multiple conditions. Here we describe such a method, using buffer equilibration followed by atomic emission spectroscopy. Simple duplex and triplex DNAs have been used to minimize site binding and structural ambiguity. The results establish this general method, define experimentally the limitations of the NLPB model, and provide a critical foundation for empirical and theoretical treatments of the ion atmosphere and its energetic consequences. This approach, in conjunction with theory, will be applicable to the energetic dissection of folding and conformational transitions and binding events involving nucleic acids and other highly charged systems.[30]

2. Experimental Section

2.1 Construction of DNA Samples. The 24-bp duplex (*24L*), duplexes with altered sequence or length (*24L*$_{alt1}$, *24L*$_{alt2}$, *44L*), and the 24-bp triplex (*T24L*) were assembled from chemically synthesized oligonucleotides (Qiagen, CA) (Supporting Information Scheme S1). Oligonucleotides were purified by ion exchange HPLC chromatography (Dionex, CA). Equimolar complementary strands were annealed in 20 mM Na-EPPS [sodium 4-(2-hydroxyethyl)piperazine-1-propanesulfonic acid, pH 8.0; for duplexes], or in 5 mM sodium acetate (pH 5.1; for the triplex), before the following buffer equilibration. Nondenaturing polyacrylamide gel electrophoresis (PAGE) with DNA staining by StainsAll (Sigma) indicated negligible contamination of free single strands (not detectable with 1 μg of annealed DNA loaded).

2.2. Ion Counting with Buffer Equilibration (BE)−Atomic Emission Spectroscopy (AES). The steps carrying out the BE−AES measurements to determine the ion atmosphere content are outlined in Figure 2 and described below (see also Supporting Information [SI] Tables S1 and S2, Figures S1−S4).

2.2.1. Buffer Equilibration. Microcon YM-30 (Millipore, MA) filters were used to carry out buffer exchange to equilibrate the DNA samples with the appropriate ionic buffer. The buffer equilibration was conducted at 4 °C. About 100 μL of DNA-containing sample is retained at the top chamber of the filter at each round of buffer exchange. Experiments at room temperature or with more extensive filtration to obtain higher concentrations and lower volumes of DNA solution gave evidence of evaporation. The evaporation is essentially eliminated in the presented protocol, as established by the absence of a significant perturbation of the buffer concentration during the exchange process (see SI Figure S2 and the accompanying text). Multiple successive buffer exchanges (6−8 rounds) were performed to ensure that the equilibrium was reached (SI Figure S3). At the end of buffer equilibration, the last 80−100 μL flow-through is collected and represents the bulk solution that the DNA-containing sample equilibrates with.

2.2.2. Determination of Ion and Phosphorous Concentrations in the Sample and Buffer by AES. Aliquots of DNA-containing sample and flow-through were diluted with water to 4 mL in polystyrene tubes (Fisher Scientific, MA). Dilution factors, the ratio of diluted sample volume (i.e., 4 mL) to the aliquot volume of DNA (20−40 μL), f_{DNA}, or flow-through (20−40 μL), f_{buffer}, were defined. The concentrations of the phosphorus (from the DNA) and ions in most of the diluted samples were within the linear dynamic range for AES detection (SI Table S1), and data that extended to the nonlinear regions were corrected based on the corresponding standard curves (SI Figure S1).

Concentrations of phosphorus and metal ions were measured simultaneously from the 4-mL samples above on an IRIS Advantage/1000 radial ICAP Spectrometer (Thermo Jarrell Ash, MA). Controls were carried out to determine the linear dynamic range and precision for each element (SI Table S1).

2.2.3. Ion Counting. The number of cations associated with (or anions depleted from) a DNA ($N_{\#ion/DNA}$) was calculated as the difference in ion concentration between the DNA-containing sample (c_{ion}^{DNA}) and its corresponding flow-through (c_{ion}^{buffer}), divided by the DNA concentration (c_{DNA}) determined by AES phosphorus measurement (eq 1). The errors shown in Figures 4, 5, 7, and 8 are the standard deviation of duplicate or triplicate measurements.

$$N_{\#ion/DNA} = \frac{c_{ion}^{DNA} - c_{\text{ion}}^{\text{buffer}}}{c_{DNA}} \tag{1}$$

Results obtained at different DNA concentrations (0.2−0.8 mM, SI Table S2) agreed within error, indicating that there are no artifacts from aggregation or intermolecular ordering.

The primary anion chloride cannot be detected directly by the spectrometer used herein. We therefore substituted chloride ion with cacodylate ion as the arsenic atom of cacodylate [$AsO_2(CH_3)_2^-$] can be detected. We verified that only anionic cacodylate (pK_a 6.3) and not the cacodylic acid was present to any significant extent in basic solution, by assessing the effect of pH on the cacodylate partitioning (SI Figure S4A). We also confirmed that there was no selective partitioning of cacodylate versus chloride that would complicate our measurements and analysis (SI Figure S4B). Thus, we determined the overall anion exclusion by linearly scaling the measured cacodylate exclusion by the reciprocal of the cacodylate abundance, $[M^-]/[AsO_2(CH_3)_2^-]$, where $[M^-]$ is the total concentration of all anion species (SI Eq. S1).

2.3. Quantitation of Cation Competition. The effectiveness of one cation species in displacing another was probed by monitoring the number of competing cations (CC) and background cations (BC) associated with the DNA over a range of concentrations of CC at a given constant concentration of BC (Figures 4, 5, 7, and 8). We define a *competition constant* as the concentration of CC at which half the number of BC associated with the DNA in the absence of a competing cation is excluded. The *competition constant* was computed as the midpoint ($[M]_{1/2}$) of BC association via a two-state model:

$$N = N_1 + \frac{(N_0 - N_1)}{1 + ([M]/[M]_{1/2})^n} \tag{2}$$

where $[M]$ is the titrated CC concentration; N_0 and N_1 are the number of associated BC at the starting and end states, respectively; n is the Hill coefficient that is parametrized simultaneously with $[M]_{1/2}$. We emphasize that this Hill analysis was carried out solely to obtain an empirical description of the competition behavior. It does not represent a physical model for ion association. Thus, the apparent Hill coefficient

simply reflects the steepness in the change of ion partition with respect to the change in ion concentration, rather than a phase transition or process that would be expected to be cooperative.

The number of associated BC was measured in the absence of CC to define the starting state and was assumed to be zero for the end state with infinite competing cation (values of the *competition constant* and *n* for the data presented in Figures 4, 5, 7 and 8 are provided in SI Table S3). The association of CC was analyzed analogously by eq 2, with the initial value assigned to be zero and a final value parametrized by the two-state fit. The fit value for the number of CC at the end states is 29−31 for monovalent and 20−22 for divalent cations. These numbers are consistent with the measurements at high CC concentrations, in the absence of significant amount of BC (e.g., 31.1 ± 2.9 in 1.2 M Na^+; 19.9 ± 0.8 in 50 mM Mg^{2+}).

2.4. NLPB Calculations. The 24- and 44-bp DNA duplex models were created with the Nucleic Acid Builder (NAB) package.[32] The 24-bp triplex model was created by axially stacking three repeats of the solution structure of an 8-bp DNA triplex (PDB ID code 1D3X) using NAB. The stacked triplexes were translated and rotated according to the average rise/base and twist/base of the triplex to achieve the continuity of the helix backbone. The protonation of cytosines (9 in total) that form the reverse Hoogsteen hydrogen bond was accounted for by assigning +1 charge to N3 of those nucleotides, giving a total charge of −65 for the 76-nucleotide long triplex (SI Scheme S1).

We solved the NLPB equation of all-atom PDB models of the DNA molecules using the Adaptive Poisson−Boltzmann Solver (APBS, ref 14 on a 192 Å × 192 Å × 336 Å grid box with spacing of 1.5 Å). We first examined the significance of the computational error from the numerical solver. The APBS solution of NLPB in cylindrical symmetry was compared to the corresponding analytical solution under salt conditions used in the experiments. The deviations in the number of associated ions were negligible (<0.1%). Further, varying the grid spacing (1.00−2.00 Å) and box size (0.66−1.33 fold of the above box dimensions) did not perturb the calculated ion numbers (<1%). The solvent and the interior of the molecule were assigned a dielectric constant of 78.54 and 2.00, respectively. Boundary conditions were obtained with the Debye−Hückel approximation. The number of ions i of valence z_i bound to the DNA was computed by integrating the excess ion density (relative to the bulk) around the DNA over all space:

$$N_i = c_i \int (e^{-z_i e\varphi/kT} - 1)\mathrm{d}V \qquad (3)$$

where e is the elementary charge, φ is the electrostatic potential, k is the Boltzmann constant, T is the temperature, and c_i is the bulk ion concentration.[9,33]

3. Results

The high surface charge density of nucleic acids attracts an ion atmosphere. Theoretical and computational methods have been used extensively to describe this atmosphere and its resultant forces,[7,10,13,34] but a quantitative and comprehensive experimental methodology to assess ion atmospheres has remained elusive.

There are several criteria for such a method. First, the method should provide as a readout a thermodynamic description of the content of the ion atmosphere, as such a description can be directly compared to predictions from theory. Equilibration by dialysis or the more rapid buffer equilibrium via centrifugation used herein meets this requirement.

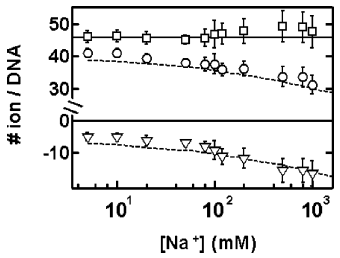

Figure 3. Neutralization of *24L* (−46 charges) by Na^+ association (○) and anion depletion (▽). The associated Na^+ ions plus the excluded anions gives the total charge of the ion atmosphere (□, solid line shows +46). Data are compared to the NLPB prediction for monovalent cations and anions (dashed lines).

Second, to read out the amount of associated ions following buffer equilibrium, the technique must be highly accurate, as identification of the composition of the ion atmosphere relies on a difference measurement (eq 1). Further, measurement of each of the ions that constitute the ion atmosphere is desired, as this information provides experimental self-consistency checks (e.g., charge neutralization of the system, see below) and provides the most extensive information for comparison with theory. Atomic emission spectroscopy (AES) meets these criteria.[35] It allows determination of the concentrations of many different ions with high precision. Unlike atomic absorption spectroscopy, AES measurements of different ions can be made simultaneously on the same sample. This decreases errors from sample-to-sample variation and minimizes the amount of sample required. Further, the amount of phosphorus atom can be measured by AES so that direct ratios of the amount of excess ions associated with the nucleic acid sample to the amount of nucleic acid present can be determined, further increasing accuracy and precision.

The protocol for buffer equilibration−atomic emission spectroscopy (BE−AES) to quantitate the ion atmosphere constituents is outlined in Figure 2 (Materials and Methods). Previously we reported in a Communication a variation of this protocol to determine site-bound Mg^{2+} ions.[27] Below we present results that provide a full accounting of the ion atmosphere surrounding simple, defined DNA duplexes and critically compare them to NLPB predictions.

3.1. The Association of the Ion Atmosphere Neutralizes the DNA Charge. Figure 3 shows the number of ions associated with the 24-bp duplex (*24L*) over a wide range of bulk Na^+ concentrations (5−1000 mM). The expectation for these data from first principles is that the system, DNA plus all ions, is charge neutral. The total charge for the ion atmosphere (squares) shows that this prediction is met; in all cases the number of associated Na^+ ions plus the excluded anions equals +46 within error (solid line; DNA charge is −46). The average total charge calculated from all the data in Figure 3 is 47.0 ± 1.4, again within error of charge neutral. The anion measurements generally have the highest uncertainty because the concentration difference for anions in the sample versus buffer is smaller than that for the cations; the signal is further reduced when the cacodylate anion is present as only a portion of the total anions present (SI Table S2 and Figure S4B). Nevertheless, the numbers

(32) Macke, T.; Case, D. A. *Molecular Modeling of Nucleic Acids*; Leontes, N. B., SantaLucia, J., Jr., Eds.; American Chemical Society: Washington, DC, 1998; pp 379−393.
(33) Sharp, K. A.; Friedman, R. A.; Misra, V.; Hecht, J.; Honig, B. *Biopolymers* **1995**, *36*, 245−262.
(34) Lyubartsev, A. P. In *Dekker Encyclopedia of Nanoscience and Nanotechnology*; Schwarz, J. A., Contescu, C. I., Putyera, K., Eds.; Marcel Dekker: New York, 2004; pp 2131−2143.
(35) Manning, T. J.; Grow, W. R. *Chem. Educ.* **1997**, *2*, 1−19.

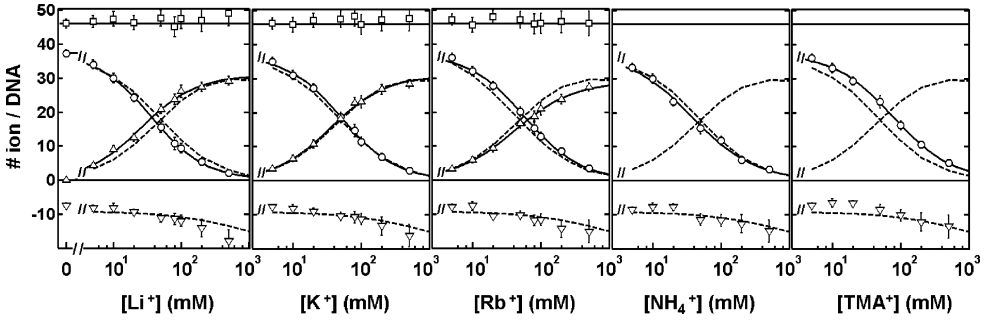

Figure 4. Competitive association of monovalent cations (Δ for Li^+, K^+ or Rb^+; NH_4^+ and TMA^+ are not detectable herein) against 50 mM Na^+ (○) for *24L*, compared with NLPB predictions (dashed lines). Data are fit with eq 2 (solid curved lines). The total charge of the ion atmosphere (□) is plotted as in Figure 3.

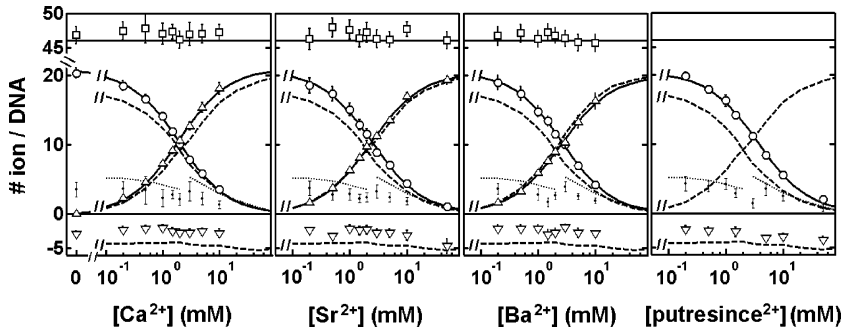

Figure 5. Competitive association of divalent cations (Δ for Ca^{2+}, Sr^{2+} or Ba^{2+}; putrescine^{2+} is not detectable by AES) against 2 mM Mg^{2+} (○) for *24L*. Data are fit to eq 2 (solid curved lines) and compared to the NLPB predictions (dashed and dotted lines). To maintain the detection accuracy of signal for the cacodylate anion, an increased concentration of sodium cacodylate (10 mM instead of 5 mM) and thus Na^+ ions was used for experiments with competing divalent ion concentrations above 2mM; this change accounts for the break in the dotted line for the Na^+ accumulation predicted by NLPB. Note that only a small amount of Na^+ (dotted points) is present in the ion atmosphere over the entire range tested conditions. The total charge of the ion atmosphere (□) is plotted as in Figure 3.

for both associated Na^+ ions and the excluded anions are in good agreement with NLPB predictions (Figure 3, dashed lines) over the tested range of Na^+ concentrations. This agreement is presumed to also hold at lower salt concentrations.[36]

The data of Figure 3 show a systematic decrease in the number of Na^+ ions and a corresponding increase in the number of excluded anions as the bulk ion concentration increases. This trend is reproduced by NLPB. This trend can be understood as follows. The DNA potential protrudes less far out into the solution at a higher ion concentration. This effect has two consequences: the associated cations that are attracted by this potential locate in a smaller volume around the DNA, thereby resulting in a higher local concentration. Furthermore, the length scale over which the concentration change between locally associated ions and the bulk concentration occurs is shorter. As a result, there is a steeper concentration gradient between the associated and the bulk cations at higher bulk concentration. Similarly, a steeper gradient of anions from near the DNA to the bulk arises with increasing salt concentration. However, the number of depleted anions is much less than that of the associated cations. Thus, the entropy increase (i.e., the concentration gradient increase) is more significant for cation association than for anion depletion. The free energy balance, therefore, favors anion depletion over cation accumulation in neutralizing DNA charge at higher salt, relative to the balance between association and exclusion at lower salt.[9,37,38]

We note that the change in the number of associated Na^+ ions (and the excluded anions) is moderate (40−35) over the wide range of Na^+ concentration (100 fold; 5−500 mM). This weak dependence of the ion accumulation on its bulk concentration is expected from first principles as there are a fixed number of charges on the DNA that need to be neutralized. It presumably arises from a counterbalancing of an increased density of Na^+ in the ion atmosphere and a sharper falloff in Na^+ density away from the DNA (see above) as the bulk Na^+ concentration is increased.[37]

The results of this and other systematic controls (SI) indicate that BE−AES can provide a full accounting of the contents of the ion atmosphere. This technique allows a fundamental thermodynamic description of all of the components of this highly charged system to be obtained.

3.2. Competitive Association of Cations: Assessing the Effects of Ion Size. NLPB theory does not take into account the effects arising from the finite ion size. This ensuing limitation of NLPB has been addressed in theoretical studies.[15,18,39] While it has been suggested experimentally that ion

(36) As discussed in the Introduction, the Manning theory, although often quoted, is a highly simplified treatment of the ion atmosphere. Manning theory partitions the ion atmosphere into "condensed" ions, directly "attached" to the macromolecule, and "mobile" ions, whose interactions are treated in a linearized Poisson−Boltzmann model. Our method measures all of the thermodynamically associated ions, which includes the "condensed" ions and contributions from the "mobile" ions in the Manning framework. Manning theory predicts the total number of excluded anions to be 0.06 ions per charge, independent of salt concentration. Experimentally, we find that the balance between associated counterions and excluded anions does change as a function of total salt concentration (Figure 3), in disagreement with the Manning prediction. Furthermore, we find that even at the lowest concentration studied (5 mM Na^+) the number of excluded anions is 0.11 ± 0.03 per charge. This indicates that even at these low ion concentrations Manning theory is, at best, approximate.

(37) Ni, H.; Anderson, C. F.; Record, M. T. *J. Phys. Chem.* **1999**, *103*, 3489−3504.
(38) Chu, B. V.; Bai, Y.; Lipfert, J.; Herschlag, D.; Doniach, S. *Biophys. J.* **2007**, *93*, 3202−3209.
(39) Bert, M. L.; Zimm, B. H. *Biopolymers* **1984**, *23*, 271−285.

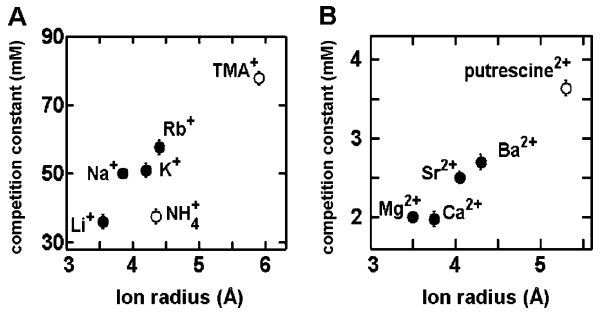

Figure 6. Competitiveness of monovalent (A) and divalent (B) cations inversely correlate with ion size. The *competition constants* are obtained from data in Figures 4 and 5 by eq 2. The radii of the hydrated ions are approximated by the distance from the ion to the water oxygen atom in the first hydration shell[44,53] plus 1.4 Å for the water layer. The radius of putrescine^{2+} is crudely estimated as half of the average separation between N atoms (the closest: 3.3 Å, the furthest: 5.5 Å) plus the radius of an amine (1.65 Å) and a water layer (1.4 Å).

size affects electrostatic screening,[22,40−42] the complexity of the systems investigated do not allow a rigorous conclusion to be drawn about the effect of ion size on its occupancy in the ion atmosphere. Thus, further experiment in a defined system was required.

The competitive association of monovalent cations or divalent cations with the 24-bp DNA duplex (*24L*) is illustrated in Figures 4 and 5, respectively. In Figure 4, the competing monovalent cations (M^+) are titrated (5 to 500 mM) into a background of 50 mM Na^+. The *competition constant* of these monovalent cations (Figure 6A) reveals a relative affinity order for occupancy of the ion atmosphere: $NH_4^+ \approx Li^+ > Na^+ \approx K^+ > Rb^+ > TMA^+$ (tetramethyl ammonium). The same preference was confirmed in an experiment against a background of 10 mM Na^+ and in a titration in which increasing concentrations of Na^+ were added to a background of 50 mM Li^+ (SI Figure S5A,B).

Figure 5 displays titrations of divalent cations (0.1−50 mM) in competition with Mg^{2+} at 2 mM. The *competition constants* for the divalent cations show a relative preference for association: $Ca^{2+} \approx Mg^{2+} > Sr^{2+} \geq Ba^{2+} >$ putrescine^{2+} (Figure 6B). The background Na^+ ions present from the buffer (5 mM if the concentration of the competing divalent salt is less than or equal to 2 mM; 10 mM otherwise) hardly participate in the ion atmosphere (1−3 per DNA). NLPB predicts more Na^+ (dotted line) and less associated divalent ions. In addition, fewer anions are excluded than the prediction (1.7 ± 0.4 on average). These results are in agreement with the findings below (see Figures 7 and 8 and the Discussion) that NLPB overestimates the association of monovalent cations and the exclusion of anions in the presence of competing divalent cations, likely because ion correlation effects that allow more accumulation of cations with higher valence are not accounted for in NLPB treatment.

Control experiments using several 24-bp DNA duplexes that contain possible specific ion-binding motifs such as A tracks and GC-rich sequences (from crystallized DNAs)[43] gave identical results (*24L*$_{alt1}$ − *24L*$_{alt2}$, SI Scheme S1 and Table S4), suggesting that effects from specific base−ion interactions or particular sequence motifs are negligible. Nevertheless, effects of binding one or a few ions at specific locations in the duplex would have been difficult to detect.

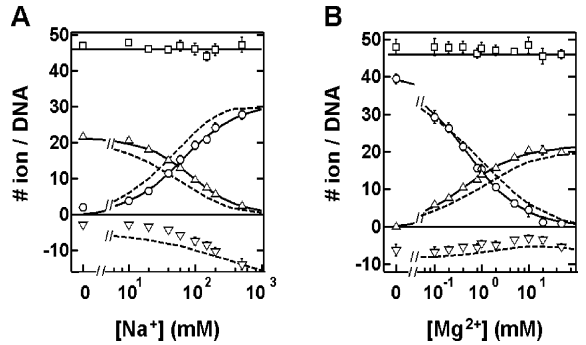

Figure 7. Competitive association between Na^+ and Mg^{2+} with *24L*. (A) Na^+ (○) was titrated into 5 mM Mg^{2+} background (Δ). (B) Mg^{2+} (Δ) was titrated into 20 mM Na^+ (○). Data are fit with eq 2 (solid curved lines) and compared to NLPB predictions (dashed lines). The total charge of the ion atmosphere (□) is plotted as in Figure 3.

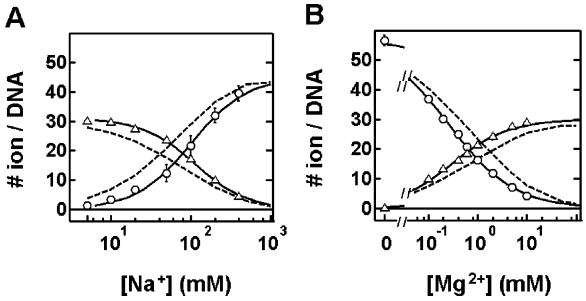

Figure 8. Competitive association of Na^+ and Mg^{2+} with the 24-bp DNA triplex (*T24L*). (A) Na^+ (○) competes with 5 mM Mg^{2+} background (Δ). (B) Mg^{2+} (Δ) competes with 20 mM Na^+ background (○). Data are fitted with eq 2 (solid curved lines) and compared to NLPB predictions (dashed lines). Anions were not detected because neutral species of cacodylate (pK_a 6.3) are present in the acidic solution (pH 5.1).

Overall, the relative affinity of the alkali and alkaline earth metal ions correlates inversely with their "sizes" (Figure 6, SI Table S5). We approximate ion sizes by their solvated radii as ions in the atmosphere generally maintain their solvation.[3] There is no perfect measure of the size of solvated radii, and indeed, ion solvation may vary in different places within the environment, and those differences may even be ion specific, especially close to a nucleic acid surface. Given these limitations, we use the radii of the first solvation shells because these values are best defined.[44] The correlation between the ion size and affinity observed in Figure 6 appears to be general and intrinsic for the ion atmosphere as it is maintained for DNAs of varying sequence, length, and surface charge (SI Table S4 and Figures S9−S10). The observed trends can be qualitatively understood by considering the effect of ion size. Large ions, to avoid overlapping with each other and with the DNA, approach the DNA less closely, resulting in weaker Coulombic interactions with the phosphates and therefore weaker screening and reduced occupancy of the atmosphere.[18,39]

Ca^{2+} has a similar affinity relative to Mg^{2+} (*competition constant* is 1.98 vs 2.0 mM), despite the larger solvation radius of Ca^{2+} (Figure 6B, 3.5 vs 3.8 Å). NMR relaxation and atomic absorption spectroscopy measurements with DNA duplexes in

(40) Strauss, U. P.; Helfgott, C.; Pink, H. *J. Phys. Chem.* **1967**, *71*, 2550−2556.
(41) Trend, B. L.; Knoll, D. A.; Ueno, M.; Evans, D. F.; Bloomfield, V. A. *Biophys. J.* **1990**, *57*, 829−834.
(42) Koculi, E.; Lee, N. K.; Thirumalai, D.; Woodson, S. A. *J. Mol. Biol.* **2004**, *341*, 27−36.
(43) Egli, M. *Chem. Biol.* **2002**, *9*, 277−286.
(44) Ohtaki, H.; Radnal, T. *Chem. Rev.* **1993**, *93*, 1157−1204.

solution and DNA fibers, respectively, suggested a preferential interaction with Ca^{2+} over Mg^{2+} [22,45] or a similar interaction with these cations.[46] Varying the GC content of the DNA duplex (37%−67%, SI Scheme S1 and Table S4) did not change the relative affinities of Ca^{2+} and Mg^{2+}, providing no indication of a base-specific enhancement of Ca^{2+} affinity, as might be anticipated from the apparent preference of inner sphere coordinations of Ca^{2+} with guanines.[43,47] Further work will be required to distinguish whether the observed preference arises from a small effective solvation radius for Ca^{2+}, from preferential interactions of solvated or partially desolvated Ca^{2+} with particular features of the DNA,[48] or from a different mechanism.

Bulkier polyions TMA^+ and $putrescine^{2+}$ are less competitive than the alkali and alkaline earth ions, respectively (Figure 6). However, ammonium exhibits a high affinity (37 mM vs 36−78 mM for the other M^+) despite its intermediate radius (4.3 Å vs 3.5−5.9 Å for the other M^+) (Figure 6A). Ammonium differs from other monovalent cations as it has protons that can hydrogen bond to acceptor atoms that are accessible in the DNA duplex, which may account for the anomalously high association of ammonium.[49]

NLPB predicts a single competition constant for all cations of the same charge (Figures 4 and 5, dashed lines), in contrast to the observed cation size effects. Thus, our experiments identify the degree of importance of and quantitate a fundamental limitation in NLPB theory. As size effects modulate electrostatic screening and thus the conformation and stability of nucleic acids and their complexes,[41,42,50] adequate treatments of the size effect in electrostatic models are necessary for an in-depth understanding of nucleic acid thermodynamics.

3.3. Competitive Association of Cations: Assessing the Effects of Ion Charge. Intensive theoretical work has suggested that the accuracy of NLPB in predicting ion association is limited by the inability of this theory to account for ion correlation, in addition to the limitations in treating ion size effects discussed above.[16,17] However, there is no straightforward and quantitative experimental benchmark for comparison of theory and experiment. As we describe below, ion correlation effects depend on the ion charge and are expected to be more important with increasing ion valency. We therefore explored the competition between monovalent and divalent cations to evaluate the accuracy of NLPB and to provide a benchmark for future theoretical treatments.

Figure 7A shows that a much higher concentration of the monovalent competitor is required to replace half of the Mg^{2+} (88 mM Na^+ vs 5 mM Mg^{2+} in Figure 7A, see also SI Figures S6 and S8A). Conversely, a concentration of only ∼0.5 mM divalent cations is required to replace half of an ion atmosphere of 20 mM Na^+ (Figure 7B and SI Figures S7 and S8B). The higher affinity of divalent cations is expected because divalent cations experience a stronger Coulombic interaction with the DNA. And fewer divalent cations are required to neutralize the DNA charge compared to monovalent ions, resulting in a smaller entropy loss accompanying divalent cation association.[9]

This preferential association of divalent cations over monovalent cations is maintained with different DNA sequences and different length duplexes, suggesting the preference is determined by the nonspecific electrostatic interactions between the ions and DNA within the accuracy of the measurements (SI Table S4, Figure S9C).

The higher affinity of divalent cations relative to that of monovalent cations is expected to favor cation association over anion exclusion in DNA neutralization, relative to the situation with monovalent cations. Accordingly, there are fewer anions excluded from the divalent cation atmosphere than from the monovalent cation atmosphere. This difference is seen most simply in Figure 7, where Na^+ is titrated into a Mg^{2+} background (e.g., -2.8 ± 0.5 in 5 mM background Mg^{2+} versus -10.4 ± 1.1 with 100 mM competing Na^+ added) and *vice versa* and also by comparison of the excluded anions in Figures 4 (-8.3 ± 0.8 to -17 ± 3.3) and 5 (-2.4 ± 0.5 to -3.9 ± 0.5).

NLPB underestimates the *competition constant* for divalent metal ions (0.48−0.57 mM observed vs 1.0 mM predicted, Figure 7B and SI Figures S7, S8B). A modified NLPB model that accounts for ion size cannot adequately account for this discrepancy.[38] Thus, a mechanism other than ion size is implicated. Theoretical studies suggest that spatial correlations of ions stabilize high cation densities close to the nucleic acid surface, resulting in a higher total cation association than that predicted by PB.[11,16,34] The correlation effects are predicted to increase with ion valence and the charge density of the polyelectrolyte.[16,17,51] Accordingly, stronger correlations and thus a larger increase of the ion occupancy relative to the NLPB prediction are expected for divalent cations over monovalent cations. Consistent with these predictions, we observe that divalent cations outcompete monovalent cations in occupying the atmosphere relative to the NLPB prediction. Along with this increased presence of divalent cations in the atmosphere, fewer anions are excluded than predicted by NLPB (Figures 5 and 7). This effect mirrors the decreased anion exclusion in the presence of divalent cations relative to monovalent cations (see above). Further, the 24-residue long triplex (*T24L*; charge of −65) with an estimated surface charge ∼40% higher than that for the 24-bp duplex (*24L*; charge of −46), gives larger deviations from NLPB predictions than the duplex, as predicted for the ion correlation effect (NLPB underestimates the competition constant of Mg^{2+} by 3- and 2-fold for the triplex and duplex, respectively; Figure 8B and SI Table S4).

4. Discussion

The ion atmosphere surrounding a nucleic acid greatly influences its structure and behavior. The association of proteins with nucleic acids, viral genome packing, and chromosomal condensation and rearrangements in replication and gene expression involve enormous electrostatic interactions that are modulated by the properties of the ion atmosphere. In-depth and complete understanding of these critical transitions of nucleic acids as isolated entities and in their biological contexts

(45) Braunlin, W. H.; Nordenskiold, L.; Drakenberg, T. *Biopolymers* **1991**, *31*, 1343−1346.
(46) Korolev, N.; Lyubartsev, A. P.; Rupprecht, A.; Nordenskiold, L. *Biophys. J.* **1999**, *77*, 2736−2749.
(47) Braunlin, W. H.; Drakenberg, T.; Nordenskiold, L. *J. Biomol. Struct. Dyn.* **1992**, *10*, 333−343.
(48) Ahmad, R.; Arakawa, H.; Tajmir-Riahi, H. A. *Biophys. J.* **2003**, *84*, 2460−2466.
(49) Hud, N. V.; Sklenar, V.; Feigon, J. *J. Mol. Biol.* **1999**, *286*, 651−660.
(50) Andresen, K.; Das, R.; Park, H. Y.; Smith, H.; Kwok, L. W.; Lamb, J. S.; Kirkland, E. J.; Herschlag, D.; Finkelstein, K. D.; Pollack, L. *Phys. Rev. Lett.* **2004**, *93*, 248103.
(51) Fixman, M. *J. Chem. Phys.* **1979**, *70*, 4995−5005.

will require an accounting of the ion atmosphere and its energetic consequences.

Nevertheless, accurate and complete determination of the ion atmosphere has been limited. As noted in the Introduction, most folding and binding studies have not provided direct assessments of ion association, and previous attempts to directly measure the ion constituents of the atmosphere have suffered from inadequate accuracy and precision, restricted range of conditions, and convolution with other processes such as folding and binding. With these limitations, the quantitative relationship between ion association and its thermodynamic consequences could not be deciphered, nor could a rigorous evaluation of the electrostatic theories of ion interactions be carried out. A direct and comprehensive accounting of the ion atmosphere was necessary.

In this work we have established a buffer equilibration−atomic emission spectroscopy approach that can quantitatively and completely dissect the contents of the ion atmosphere. The competitive association of monovalent and divalent cations with simple, well-defined DNA molecules has been systematically and quantitatively explored.

The relative association of monovalent or divalent cations exhibits an inverse correlation with ion size (Figures 4, 5, and 6). This size effect is maintained for DNA molecules of varying length, surface charge, and base composition (SI Tables S4 and S5, Figures S9 and S10), suggesting that ion size affects the composition of the ion atmosphere nonspecifically. The anion exclusion appears to be insensitive to ion size, as observed by the consistency of results with varying ratios of cacodylate versus chloride ions (SI Figure S4B and accompanying text).

The competition constant of divalent cations in the presence of monovalent cations (and *vice versa*) quantitatively demonstrates the much stronger competitiveness of divalent cations. For example, a competition constant of 0.48 mM for Mg^{2+} in 20 mM Na^{+} indicates that Mg^{2+} ions associate 40-fold more strongly than Na^{+} ions in the atmosphere (Figure 7B). Moreover, divalent ions outcompete monovalent ions for ion atmosphere occupancy relative to the NLPB prediction, a discrepancy that is consistent with a significant contribution from ion correlation effects that are omitted in the NLPB mean field treatment.

Although the limitations of NLPB in the treatment of ion sizes and correlations have been extensively discussed,[15,17,18,34,39,52] the actual extent of these limitations was not previously known and has been quantitatively revealed for the first time in this work. The observed deviations are larger for divalent than for monovalent cations (Figures 4 and 7), larger for a polyamine than for a small spherical metal ion (Figures 5 and 6B), and larger with nucleic acids of higher charge density (Figure 8, SI Table S4). These trends confirm the predicted limitations of NLPB as a mean-field theory.[16−18,37,52] More importantly, quantitation of the ion atmosphere will provide explicit guidance in selecting appropriate electrostatic treatments and in developing more accurate electrostatic theories.[38] One particularly difficult area for theory is the treatment of polyamines, such as putrescine^{2+} (Figure 5 and 6B). Polyamines are abundant as biological counterions but difficult to treat theoretically as they lack spherical symmetry and can adopt a range of distances between the intramolecular amines.

The approach herein, BE−AES, is readily applicable to a wide range of thermodynamic studies of nucleic acids and other highly charged systems. Such studies, in conjunction with improved computational methods developed with these and other studies as a guide, should allow parsing of the thermodynamic contributions to complex and biologically important equilibria, such as the folding of functional RNAs and the association of proteins with RNA and DNA targets.

Acknowledgment. We are indebted to the expert advice and technical assistance of Guangchao Li of the Stanford Geological and Environmental Science Department for the instrumental analysis throughout this work. We also thank Mark Engelhardt, Vijay Pande, and members of the Herschlag lab for useful discussions. Funding was provided by Stanford Graduate Fellowship (Y.B.), a Pfizer Bio-X Graduate Student Fellowship (V.C.), and an NIH Grant PO1-GM066275 and Stanford Bio-X Grant (D.H. and S.D.).

Supporting Information Available: The linear dynamic range and precision of AES spectrometer; controls determining equilibration between the DNA-containing sample and the buffer; validation of measuring anion exclusion by cacodylate substitution; examples of determining the ion atmosphere from BE−AES measurements; competitive ion association with DNA duplexes of varying sequence and length and with a DNA triplex. This material is available free of charge via the Internet at http://pubs.acs.org.

JA075020G

(52) Lamm, G.; Wong, L.; Pack, G. R. *Biopolymers* **1994**, *34*, 227−237.
(53) Garde, S.; Hummer, G.; Paulaitis, M. E. *J. Chem. Phys.* **1997**, *108*, 1552−1561.